Functional network integrity presages cognitive decline in preclinical Alzheimer disease

Rachel F. Buckley, PhD*
Aaron P. Schultz, PhD*
Trey Hedden, PhD
Kathryn V. Papp, PhD
Bernard J. Hanseeuw, MD, PhD
Gad Marshall, MD
Jorge Sepulcre, MD, PhD
Emily E. Smith, BS
Dorene M. Rentz, PhD
Keith A. Johnson, MD
Reisa A. Sperling, MD
Jasmeer P. Chhatwal, MD, PhD

Correspondence to Dr. Sperling: reisa@bwh.harvard.edu

ABSTRACT

Objective: To examine the utility of resting-state functional connectivity MRI (rs-fcMRI) measurements of network integrity as a predictor of future cognitive decline in preclinical Alzheimer disease (AD).

Methods: A total of 237 clinically normal older adults (aged 63–90 years, Clinical Dementia Rating 0) underwent baseline β-amyloid (Aβ) imaging with Pittsburgh compound B PET and structural and rs-fcMRI. We identified 7 networks for analysis, including 4 cognitive networks (default, salience, dorsal attention, and frontoparietal control) and 3 noncognitive networks (primary visual, extrastriate visual, motor). Using linear and curvilinear mixed models, we used baseline connectivity in these networks to predict longitudinal changes in preclinical Alzheimer cognitive composite (PACC) performance, both alone and interacting with Aβ burden. Median neuropsychological follow-up was 3 years.

Results: Baseline connectivity in the default, salience, and control networks predicted longitudinal PACC decline, unlike connectivity in the dorsal attention and all noncognitive networks. Default, salience, and control network connectivity was also synergistic with Aβ burden in predicting decline, with combined higher Aβ and lower connectivity predicting the steepest curvilinear decline in PACC performance.

Conclusions: In clinically normal older adults, lower functional connectivity predicted more rapid decline in PACC scores over time, particularly when coupled with increased Aβ burden. Among examined networks, default, salience, and control networks were the strongest predictors of rate of change in PACC scores, with the inflection point of greatest decline beyond the fourth year of follow-up. These results suggest that rs-fcMRI may be a useful predictor of early, AD-related cognitive decline in clinical research settings. *Neurology*® 2017;89:29–37

GLOSSARY

Aβ = β-amyloid; **AD** = Alzheimer disease; **AIC** = Akaike information criteria; **ANOVA** = analysis of variance; **BIC** = Bayesian information criteria; **DVR** = distribution volume ratio; **FC** = functional connectivity; **FCSRT** = Free and Cued Selective Reminding Test; **FLR** = frontal, lateral, and retrosplenial tracer uptake; **GM** = gray matter; **HABS** = Harvard Aging Brain Study; **ICV** = intracranial volume; **LM-DR** = Logical Memory IIa delayed recall; **MMSE** = Mini-Mental State Examination; **MNI** = Montreal Neurological Institute; **PACC** = Preclinical Alzheimer Cognitive Composite; **PiB** = Pittsburgh compound B; **rs-fcMRI** = resting-state functional connectivity; **TBR** = template-based rotation analysis; **TE** = echo time; **TR** = repetition time.

Though assessment of β-amyloid (Aβ) burden is critical to the conceptualization of preclinical Alzheimer disease (AD), the presence of elevated Aβ alone is associated with variable levels of cognitive decline. It is now widely accepted that supplementing Aβ status with a marker of neurodegeneration or tau burden is likely a critical step in achieving this end.[1,2] In the current study, we focused on the ability of resting-state functional connectivity (rs-fcMRI) to provide evidence of early intrinsic network disconnectivity that may predict future cognitive decline in older adults, either alone or in concert with Aβ.

Supplemental data at Neurology.org

*These authors contributed equally to this work.

From the Florey Institutes of Neuroscience and Mental Health (R.F.B.), Melbourne; Melbourne School of Psychological Science (R.F.B.), University of Melbourne, Australia; Department of Neurology (R.F.B., A.P.S., K.V.P., B.J.H., G.M., D.M.R., K.A.J., R.A.S., J.P.C.), Athinoula A. Martinos Center for Biomedical Imaging (A.P.S., T.H., B.J.H., J.S., K.A.J.) and Gordon Center for Medical Imaging, Division of Nuclear Medicine and Molecular Imaging (J.S., K.A.J.), Department of Radiology, Massachusetts General Hospital; Harvard Medical School (R.F.B., A.P.S., T.H., K.V.P., B.J.H., G.M., D.M.R., K.A.J., R.A.S., J.P.C.); Center for Alzheimer Research and Treatment, Department of Neurology (K.V.P., G.M., D.M.R., K.A.J., R.A.S., J.P.C.), Brigham and Women's Hospital, Boston, MA: and Department of Psychiatry (E.E.S.), University of Texas Southwestern Medical Center, Dallas.

Go to Neurology.org for full disclosures. Funding information and disclosures deemed relevant by the authors, if any, are provided at the end of the article.

Cognitive decline has been associated with brain network alterations in rs-fcMRI of the default network in patients with AD dementia.[3–5] Decreases in default network connectivity are also seen with increasing clinical impairment from mild cognitive impairment to clinically evident AD dementia,[3,6,7] and the default network is among the sites of early Aβ deposition in AD.[4,8] Recent studies suggest that other cognitive rs-fcMRI networks, especially the salience, dorsal attention, and frontoparietal control networks, are also targeted in AD.[9] We examined the hypothesis that disruptions in network integrity measurable by rs-fcMRI predict future cognitive decline in a longitudinal cohort of clinically normal elderly participants. We further hypothesized that the predictive effect of reduced network connectivity would be synergistic with neocortical Aβ burden, with the steepest cognitive decline evident in individuals with higher Aβ burden and reduced rs-fcMRI.

METHODS

Participants. A total of 237 clinically normal participants from the Harvard Aging Brain Study (HABS) underwent baseline neocortical Aβ imaging with Pittsburgh compound B (PiB) PET imaging and structural and resting-state functional MRI (PiB-MRI interval = 158 ± 97 days; relatively slow amyloid accumulation reported in the literature[10] supports this time interval as acceptable). To be enrolled in the HABS study, participants needed to score 0 on the Clinical Dementia Rating Scale global score, greater than 25 on the Mini-Mental State Examination, and less than 11 on the Geriatric Depression Scale, and to perform within validated education-adjusted norms on Logical Memory II delayed recall. Twenty-six participants (4%) were left-handed. To be included in this study, participants were additionally required to possess at least 2 annual neuropsychological assessments: 9 completed 2 visits, 58 completed 3 visits, 37 completed 4 visits, 75 completed 5 visits, and 58 completed 6 visits. The median neuropsychological follow-up period was 3 years. Baseline demographics can be found in table 1.

Standard protocol approvals, registrations, and patient consents. Study protocols were approved by the Partners Healthcare Institutional Review Board and all participants provided written informed consent.

MRI. MRI were collected on a 3T Trio Tim scanner (Siemens Medical Systems, Erlangen, Germany) using 12-channel phased-array head coils. fMRI data were acquired using a gradient-echo echoplanar imaging sequence sensitive to blood oxygen level–dependent contrast. Whole-brain coverage was acquired using repetition time (TR) 3 seconds, flip angle 85°, echo time (TE) 30 ms, matrix 72 × 72, field of view 216 × 216 mm, and 47 × 3 mm axial slices, which resulted in isotropic voxels of 3 mm. Two 124 volumes were acquired in 2 6:12 runs for a total of 12:24. A crosshair was projected on a screen visible to participants during the scan, and participants were asked to lie flat, keep eyes open, and remain awake.

We processed resting-state data using SPM8 (fil.ion.ucl.ac.uk/spm/). We excluded the first 4 volumes of each run for T1 equilibration. We slice-time corrected each run (using fifth order or polynomial splines, with the first slice as the reference slice), realigned to the first volume of each run with INRIAlign, and normalized each run nonlinearly to the Montreal Neurological Institute (MNI) 152 EPI template (using statistical parametric mapping–defined normalization parameters). This was conducted to avoid warping artifact that can occur when normalizing to the T1 image. We smoothed with a 6-mm Gaussian kernel, as

Table 1 Baseline demographic and cognitive measures according to β-amyloid (Aβ) status

	Overall (n = 237), mean (SD)	Aβ− (n = 181), mean (SD)	Aβ+ (n = 55), mean (SD)	p Value
Demographics				
Age, y	73.4 (6.0)	72.7 (5.9)	75.7 (5.5)	<0.001
Education, y	15.8 (3.0)	15.6 (3.1)	16.5 (2.6)	0.05
% Female	60	59	61	0.67
PiB FLR DVR	1.16 (0.2)	1.08 (0.1)	1.41 (0.1)	<0.001
Aβ, % high burden	23	—	—	—
APOE ε4, % carrier[a]	29	20	61	<0.001
Cognitive performance				
MMSE	28.9 (1.1)	29.0 (1.1)	28.8 (1.1)	0.29
LM delayed recall	13.7 (3.2)	13.6 (3.2)	13.7 (3.2)	0.72
Digit symbol	47.1 (10.8)	47.0 (10.8)	47.0 (10.8)	0.98
FCSRT total score	47.6 (0.9)	47.6 (0.9)	47.6 (0.9)	0.61
FCSRT free recall	33.3 (5.4)	33.4 (5.4)	33.4 (5.4)	0.94

Abbreviations: DVR = distribution volume ratio; FCSRT = Free and Cued Selective Reminding Test; FLR = frontal, lateral, and retrosplenial tracer uptake; LM = Logical Memory; MMSE = Mini-Mental State Examination; PiB = Pittsburgh Compound B.
[a] No. = 223.

Figure 1 Model estimates of Preclinical Alzheimer Cognitive Composite (PACC) decline according to resting-state functional connectivity networks

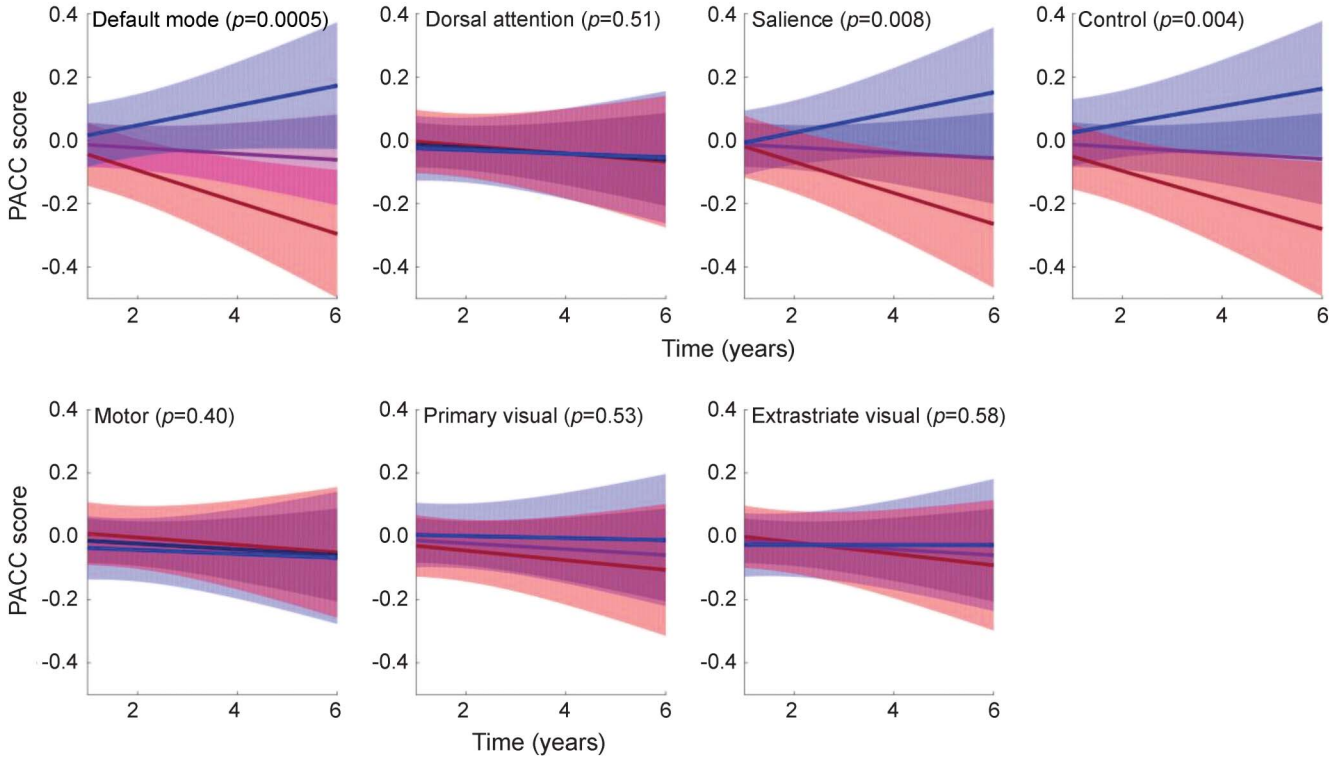

Slopes represent PACC trajectories according to connectivity in all functional networks. Blue line indicates baseline connectivity 1 SD above the group mean (i.e., high connectivity); purple line indicates mean baseline connectivity; red line indicates baseline connectivity 1 SD below the group mean (i.e., low connectivity).

this boosts the signal-to-noise ratio and improves intersubject registration. Additional processing included (1) movement correction using the coregistration parameters (plus first derivatives) in order to reduce movement artifacts and (2) temporal bandpass filtering to remove frequencies outside of the 0.01–0.08 Hz band. Further details can be found at Schultz et al.[11] In addition, outlier volumes were scrubbed from the connectivity analysis if change in global signal was more than 2.5 SDs from the mean change, if change in position was greater than 0.75 mm from the previous volume, or if change in rotation was greater than 1.5° from the previous volume. Individual runs were dropped if more than 20 volumes in a run were flagged as outliers (n = 2) or if the average temporal signal to noise was less than 115 (n = 1).

Template maps for the default mode, salience, dorsal attention, frontoparietal control, primary visual, extrastriate visual, and motor networks were derived from an out-of-sample population of 675 participants in the Brain Genomics Superscript Project[12] (neuroinformatics.harvard.edu/gsp/). Participants were an average of 21 years old (range 18 and 35 years), and were 58% female, 12% left-handed, with approximately 14 years of education.[11,13] These demographics did not substantially depart from a recent publication of the larger study cohort.[13] Derivation, reproducibility, and use of these templates to generate connectivity measures have previously been described in detail.[11,14] Maps and relevant code for template-based rotation analysis (TBR) are publicly available at mrtools.mgh.harvard.edu. TBR connectivity measures for each participant and each network were calculated by computing the average correlation strength of all voxels within a particular thresholded network mask (threshold defined as greater than 40% of the maximum value in the corresponding template map), yielding a whole network average connectivity measure. The default network comprised an aggregate of posterior midline, parietal, medial frontal, lateral temporal, and parahippocampal regions,[11] similar to previous reports of this network.[15,16] Although some studies have fractionated the default mode into subnetworks[17,18] (particularly anterior and posterior or ventral and dorsal subsystems), our unified default network accords well with prior work using seed-based analyses[19] and group independent component analysis,[18] and is highly similar to the parcellation arrived at via cluster analysis.[15] Notably, we have demonstrated that connectivity measures derived using this unified default network template are significantly related to cognitive performance in the HAB study.[14] The salience network is predominantly composed of dorsal anterior cingulate, prefrontal, frontal, and insula regions, and is similar to that reported by Seeley et al.[16] The dorsal attention network, including the parietal and fusiform regions, closely mirrors that of Yeo et al.[15] MNI seeds for all templates can be found in our methods publication.[11]

Structural T1-weighted images were acquired as magnetization-prepared rapid gradient echo with the following acquisition parameters: TR/TE/inversion time 2,300/2.95/900 ms, flip angle 9°, 1.1 × 1.1 × 1.2 mm resolution, 2 × (GRAPPA) acceleration. The structural MRI data were processed with Freesurfer v5.1. For the current study, total gray matter (GM) volume was used as a covariate, and was adjusted according to each individual's estimated total intracranial volume (ICV) (GM and white matter measured) using the following algorithm:

$$GM_{adjusted} = \text{Raw GM} - b \times (\text{ICV} - \text{Mean ICV})$$

where b indicates the regression coefficient when GM is regressed against ICV.[1]

Figure 2 Model estimates of Preclinical Alzheimer Cognitive Composite (PACC) slopes

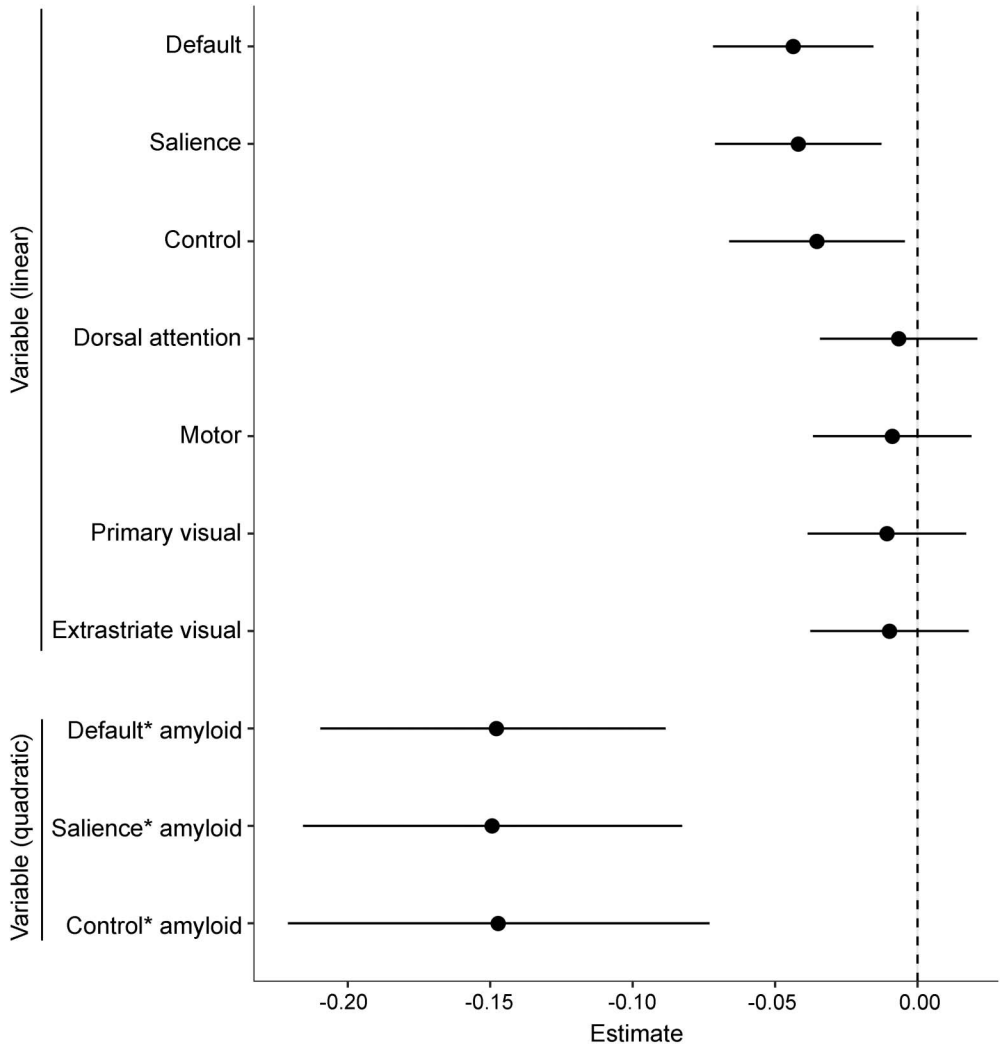

Above the horizontal line: estimates of the linear slopes of cognitive decline according to each resting-state functional connectivity network. Below the horizontal line: estimates of the quadratic slopes of cognitive decline according to the interaction between β-amyloid (Aβ) and default mode/salience/frontoparietal networks. Estimate represents the change in PACC (by SD/year) according to a unit increase in network disconnectivity (above horizontal line) or a unit increase in the Aβ × network disconnectivity interaction (below the horizontal line).

PET imaging. Acquisition of ^{11}C PiB-PET data in HABS has previously been described in detail.[20] In brief, PiB-PET images were acquired with an 8.5–15 mCi bolus injection and a subsequent 1-hour dynamic acquisition over 69 volumes (12 × 15 seconds, 57 × 60 seconds). PET data underwent reconstruction and attenuation correction, were evaluated for head motion, and were coregistered to the corresponding T1 image for each participant using a 6 degrees of freedom rigid body registration. Further details on our PET methodology can be found in our previous publication.[21] A summary distribution volume ratio (DVR) of frontal, lateral, and retrosplenial tracer uptake (FLR),[22] as defined by Freesurfer v5.1, was calculated for each participant by averaging the median PiB uptake value across voxels in the precuneus, rostral anterior cingulate, medial orbito-frontal, superior frontal, rostral middle frontal, inferior parietal, inferior temporal, and middle temporal regions of interest from both hemispheres divided by the median PiB DVR from cerebellar GM. The regions comprising the FLR are known to show elevated PiB binding in AD dementia patients.[23] The cutoff of PiB FLR DVR >1.2 for Aβ positivity was derived via a Gaussian mixture model approach detailed in a prior report.[1]

Cognitive measures. The Preclinical Alzheimer Cognitive Composite (PACC) was created using the following neuropsychological tests[24]: the Logical Memory IIa delayed recall (LM-DR) index from the Wechsler Memory Scale,[25] the Mini-Mental State Examination (MMSE) total score,[26] the Digit Symbol Substitution Test score from the Wechsler Adult Intelligence Scale–Revised,[27] and a combined summation of the Free and Cued Selective Reminding Test (FCSRT) free recall and total recall (free + cued) indices.[28] Measures were *z* score transformed based on the mean (SD) from baseline data and averaged, with a higher score on the PACC indicating better performance. For the current study, each of the measures were also examined as dependent variables to determine which components of the PACC might be most strongly related to functional connectivity (FC) networks.

Analyses. We used the nlme statistical package in R (version 3.3.0) software to implement linear and nonlinear mixed models.

Figure 3 3D representation of the rate of change of Preclinical Alzheimer Cognitive Composite (PACC) over time according to default network connectivity and level of β-amyloid (Aβ) burden

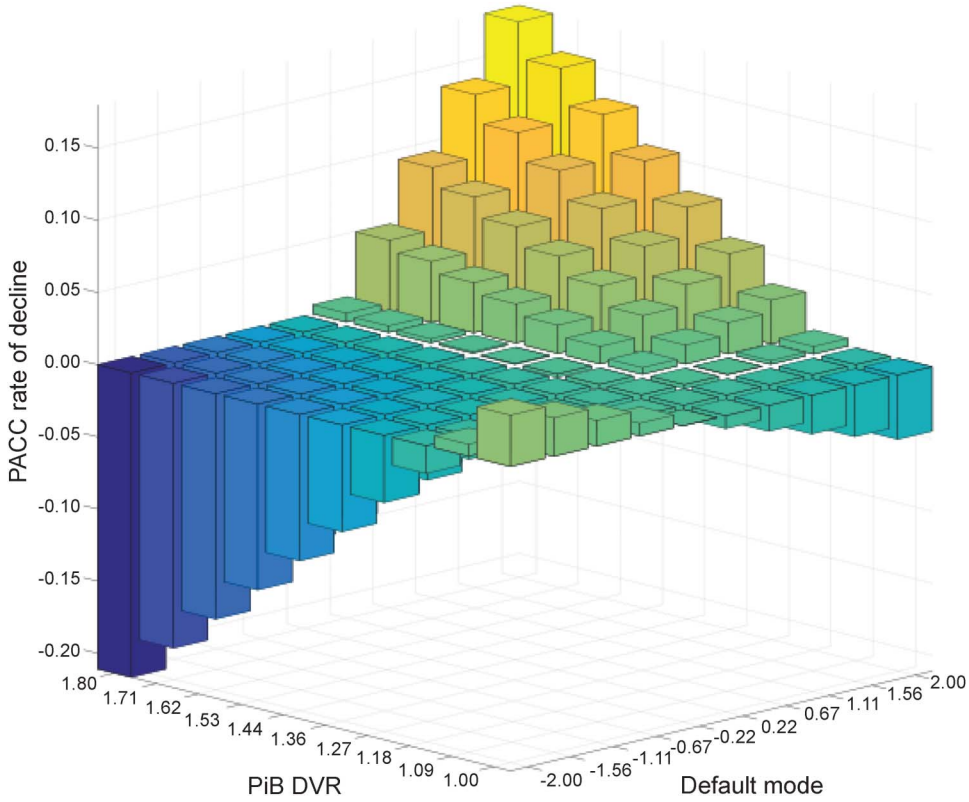

Each bar represents rate of PACC change according to default network connectivity (x axis) and Aβ burden (z axis), with rates of change in PACC slope (on the y axis) represented by each bar in the figure. Darker blue bars indicate greater rates of PACC decline (evidenced in cases of highest Aβ burden and lowest default connectivity), while lighter yellow bars indicate practice effects. PiB DVR = Pittsburgh compound B distribution volume ratio.

Models were constructed to ascertain the influence of FC networks and Aβ on longitudinal PACC performance or on the PACC components. Both random effects of intercept and slope for each participant were modeled using maximum likelihood estimation, with linear and quadratic terms for time. For each FC network, we examined the same set of models:

1. Cognition ~ time + covariates × time
2. Cognition ~ FC_network × time + covariates × time
3. Cognition ~ FC_network × Aβ × time + covariates × time
4. Cognition ~ FC_network × Aβ × time + FC_network × Aβ × time^2 + covariates × time

Cognition = PACC (within the PACC: MMSE, LM-DR, Digit Symbol, or FCSRT)

Covariates = age, years of education, $GM_{adjusted}$

The fit of each increasingly complex model was tested against the fit of the prior model using analysis of variance (ANOVA). A more complex model was rejected in favor of a simpler model if the ANOVA revealed $p > 0.05$. Differences in the fit indices were reported as the difference in Akaike information criteria (ΔAIC) and the difference in Bayesian information criteria (ΔBIC) between the 2 models. Only significant covariate-by-time interactions were included in final models. Whole network connectivity measurements were regressed against movement and number of outlier volumes and z scored prior to inclusion into the models above. Multiple independent comparisons were accounted for according to a Sidak correction of $\alpha = 0.007$. For ease of interpretation of the continuous rs-fcMRI and Aβ predictors, our figures represent model estimates of cognitive slopes according to differing levels of connectivity or Aβ burden.

RESULTS FC networks on PACC change. Baseline PACC scores were weakly positively associated with baseline default network, $r(235) = 0.16$, $p = 0.01$, salience, $r(235) = 0.15$, $p = 0.02$, and control network connectivity, $r(235) = 0.2$, $p = 0.001$. According to model 2, lower baseline default, salience, and control network functional connectivity at enrollment in the study was associated with PACC decline over time, even after accounting for covariates (age, education, GM volume). By contrast, dorsal attention network connectivity was not a significant predictor of longitudinal PACC performance. Connectivity in the sensory networks, primary visual, motor, and extrastriate visual, also did not predict change in PACC scores over time (see table e-1 at Neurology.org for details). These results suggest that the effect of connectivity on the PACC is limited to a subset of cognitive networks. As default, salience, and control networks showed the clearest relationship with PACC score decline, further analyses were conducted using only these networks. A diagrammatic depiction of the

Figure 4 Nonlinear model estimates of Preclinical Alzheimer Cognitive Composite (PACC) slopes according to default, salience, or control networks by β-amyloid (Aβ) interaction

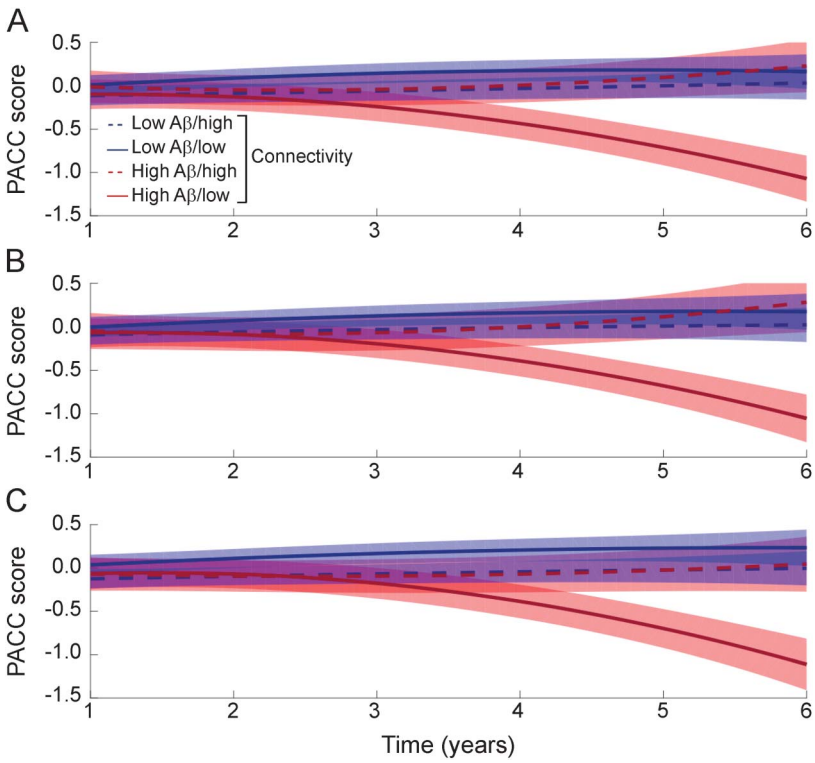

Slopes represent nonlinear trajectories according to different levels of Aβ burden and network connectivity in (A) default, (B) salience, and (C) control networks; low Aβ burden ($M_{PiB\ DVR}$ = 1.08), high Aβ burden ($M_{PiB\ DVR}$ = 1.40), low default connectivity ($M_{Below\ median\ split\ across\ networks}$ = −0.77), high default connectivity ($M_{Above\ median\ split\ across\ networks}$ = 0.78). Error bars are 95% confidence interval. PiB DVR = Pittsburgh compound B distribution volume ratio.

model slopes for each network can be found in figure 1A; forest plot of the slope estimates can be found in figure 2 (with full model estimates and effect sizes in table e-1).

Interaction between default, salience, and control network connectivity and Aβ on PACC change. As the PACC was developed to be a sensitive measure of Aβ-related cognitive decline,[24] we hypothesized that interactions between Aβ and default network connectivity would significantly predict PACC decline. In this context, we next modeled longitudinal PACC scores by including 3-way linear and quadratic interactions between default, salience, or control networks and Aβ burden with time. While both linear and quadratic time interaction terms were significant predictors of PACC change (table e-1), inclusion of a quadratic term improved model fit as compared with the linear-only model for all 3 networks examined (default network: model 3 vs 4: ΔAIC = 18.4, ΔBIC = −1.17, log-likelihood ratio = 13.2, $p < 0.0001$). An illustrative depiction of this 3-way interaction can be found in figure 3.

Considering the quadratic model, we observed that lower baseline default network connectivity interacted with higher Aβ burden to predict poorer PACC scores over time (see figure 3). The improved model fit came as a result of a quadratic inflection at the third year of follow-up, with poorer default network connectivity and higher Aβ burden relating to rapidly declining PACC scores after this point (refer to figure 4A). By contrast, in individuals with low Aβ burden, no influence of default network connectivity was found on longitudinal PACC scores. Similar quadratic interactions were found between salience network and Aβ (figure 4B), and control network and Aβ (figure 4C), again with a quadratic inflection at the third year of follow-up. Tables e-2 and e-3 present the estimates for the linear-only and full quadratic models, respectively. Figures e-1 and e-2 depict the raw data of PACC score change over time.

Default network and Aβ on change in individual measures comprising the PACC. We next decomposed the PACC into its 4 constituent measures and assessed the longitudinal relationship of each to baseline default network connectivity. Three-way interactions among default network connectivity, Aβ, and time significantly predicted longitudinal FCSRT total, MMSE, and Digit Symbol Substitution scores. Furthermore, models including quadratic time terms fit significantly better than similar linear models. Longitudinal FCSRT free recall performance showed a similar pattern (model 4, default × Aβ × time^2 term, $p = 0.06$). The 3-way interaction also significantly predicted longitudinal Logical Memory delayed recall performance, though for this measure the fit of linear and quadratic models was statistically similar (model 3 vs 4: ΔAIC = −0.92, BIC = −20.50, log-likelihood ratio = 7.08, $p = 0.13$). For Logical Memory, those with low Aβ burden showed a clear practice effect, whereas a lack of evident practice effect was seen in individuals with combined higher Aβ burden and lower default network connectivity (see table e-4 and figure e-2).

DISCUSSION Our results add to a body of literature demonstrating relationships between Aβ burden and rs-fcMRI measures of network connectivity (particularly with respect to the default,[4,9,20,29–31] salience, and control networks), and further suggest that connectivity measures across cognitive networks can act synergistically with Aβ burden to predict cognitive decline in preclinical AD. Previous studies indicate that Aβ preferentially aggregates in areas of high intrinsic connectivity,[30] especially in the default network.[8,32] In individuals with high Aβ burden, lower cognitive network connectivity may represent evidence of Aβ-related synaptic dysfunction,[33] suggesting these individuals are further along the pathway to

AD-related cognitive decline.[34] Alternatively, measures of intrinsic connectivity may serve as an Aβ-independent marker of reserve capacity,[5,35] such that individuals with lower levels of connectivity (and, potentially, lower reserve) may be more susceptible to Aβ-related cognitive decline. More broadly, the results motivate further studies focusing on the relationship between connectivity and reserve, including metrics of brain[36] and cognitive reserve (i.e., education, premorbid intelligence, occupational attainment, cognitive activities, or some combination of these).[37]

In addition to the heavily studied default network, we found that altered connectivity in the salience and control networks was predictive of Aβ-related cognitive decline. These relationships were subtly weaker than with the default network, though the overall patterns with respect to linear and quadratic slopes of PACC decline were similar. This result is perhaps unsurprising given that these networks show relationships similar to the default network with respect to performance on executive and episodic memory tests,[14] and are also thought to be susceptible to disruption by early Aβ deposition.[9,38] Further evidence for cognitive network specificity in the prediction of cognitive decline was provided by the null result when examining the influence of visual or motor networks as predictors of longitudinal PACC scores. Notably, previous studies have not found a relationship between connectivity in visual and motor networks and Aβ burden.[31]

It remains uncertain whether disconnectivity of intrinsic networks appears prior to Aβ deposition, as suggested by recent studies,[3] or whether the connectivity changes are a consequence of abnormal protein deposition in nodes within targeted networks.[33,39] This question is further complicated by studies suggesting that hyperactivity and hyperconnectivity within affected networks may precede a later stage of disease in which progressive declines in connectivity mirror progressive cognitive decline.[29] If present, hyperconnectivity and hyperactivity in targeted networks[30] may reflect early Aβ-induced alterations in neural processing, and this increased activity may itself promote further production of toxic Aβ species. Longitudinal rs-fcMRI studies will address these questions, and help elucidate cause-and-effect relationships between Aβ deposition and changes in connectivity.

Generalizability beyond the demographic characteristics of the cohort and the potential for attrition bias are possible limitations of the present study. The HABS cohort has relatively high levels of education and performance on verbal IQ testing, and, accordingly, the levels of cognitive reserve in this cohort may affect the observed levels of connectivity and pattern of cognitive decline. In addition, some participants did not complete all follow-up assessments, and considering that individuals with cognitive impairment are more likely to drop out of longitudinal studies,[40] it is possible that systematic attrition of this type may lead to an underestimation of baseline rs-fcMRI and Aβ as predictors of cognitive decline.

Our results indicate that early evidence of intrinsic network dysfunction, especially in the setting of co-occurring AD pathology, may presage future cognitive decline. The demonstrable synergy between connectivity and Aβ burden in predicting decline suggests that connectivity measurements may complement imaging biomarkers of AD pathology by helping to distinguish individuals who are more (low connectivity) or less (high connectivity) susceptible to progressive, pathology-induced cognitive decline. Though further work is needed to operationalize connectivity measurements and to establish reliable cutoffs, the results here also suggest that rs-fcMRI could potentially be integrated with other available biomarkers to improve the identification of individuals at the highest risk of impending cognitive decline.

AUTHOR CONTRIBUTIONS

Rachel Buckley, Aaron Schultz, Jasmeer Chhatwal: study concept and design. All authors: acquisition of data. Rachel Buckley, Aaron Schultz, Reisa Sperling, Jasmeer Chhatwal: analysis and interpretation of data. Reisa Sperling, Keith Johnson: study supervision. All authors: critical revision of manuscript for intellectual content.

STUDY FUNDING

Dr. Buckley is funded by the NHMRC Dementia Research Fellowship (APP1105576). This work was supported with funding from the NIH, including P01 AG036694 (R.A.S., K.A.J.), P50 AG005134 (R.A.S., K.A.J., T.H.), K23 EB019023 (J.S.), K23 AG049087 (J.P.C.), K24 AG035007 (R.A.S.), and K01 040197 (T.H.). This research was carried out in part at the Athinoula A. Martinos Center for Biomedical Imaging at the Massachusetts General Hospital, using resources provided by the Center for Functional Neuroimaging Technologies, P41EB015896, a P41 Biotechnology Resource Grant supported by the National Institute of Biomedical Imaging and Bioengineering, NIH. This work also involved the use of instrumentation supported by the NIH Shared Instrumentation Grant Program and/or High-End Instrumentation Grant Program; specifically, grants S10RR021110, S10RR023401, and S10RR023043.

DISCLOSURE

R. Buckley is funded by the NHMRC Dementia Research Fellowship (APP1105576). A. Schultz has been a paid consultant for Janssen Pharmaceuticals and Biogen. T. Hedden is funded by NIH (K01 040197). K. Papp has been a paid consultant for Biogen. B. Hanseeuw is funded by the Belgian American Education Foundation (BAEF), Belgian National Fund for Scientific Research (FNRS), and Saint-Luc Foundation. G. Marshall has received research salary support from Eisai Inc. and Eli Lilly and Company. J. Sepulcre is funded by NIH (K23 EB019023). E. Smith reports no disclosures relevant to the manuscript. D. Rentz served as a consultant for Eli Lilly, Biogen Idec, and Lundbeck Pharmaceuticals, and serves as a member of the Scientific Advisory Board for Neurotrack. K. Johnson has served as a paid consultant for Bayer, GE Healthcare, Janssen Alzheimer's Immunotherapy, Siemens Medical Solutions, Genzyme, Novartis, Biogen, Roche, ISIS Pharma, AZTherapy, GEHC, Lundberg, and Abbvie. He is a site coinvestigator for Lilly/Avid, Pfizer, Janssen Immunotherapy, and Navidea. He has spoken at symposia

sponsored by Janssen Alzheimer's Immunotherapy and Pfizer. K. Johnson receives funding from NIH grants R01EB014894, R21 AG038994, R01 AG026484, R01 AG034556, P50 AG00513421, U19 AG10483, P01 AG036694, R13 AG042201174210, R01 AG027435, and R01 AG037497 and the Alzheimer's Association grant ZEN-10-174210. R. Sperling has served as a paid consultant for Abbvie, Biogen, Bracket, Genentech, Lundbeck, Roche, and Sanofi. She has served as a coinvestigator for Avid, Eli Lilly, and Janssen Alzheimer Immunotherapy clinical trials. She has spoken at symposia sponsored by Eli Lilly, Biogen, and Janssen. R. Sperling receives research support from Janssen Pharmaceuticals and Eli Lilly and Co. These relationships are not related to the content in the manuscript. She also receives research support from the following grants: P01 AG036694, U01 AG032438, U01 AG024904, R01 AG037497, R01 AG034556, K24 AG035007, P50 AG005134, U19 AG010483, R01 AG027435, Fidelity Biosciences, Harvard Neuro-Discovery Center, and the Alzheimer's Association. J. Chhatwal is funded by NIH (K23 AG049087). Go to Neurology.org for full disclosures.

Received November 22, 2016. Accepted in final form March 29, 2017.

REFERENCES

1. Mormino EC, Betensky RA, Hedden T, et al. Synergistic effect of β-amyloid and neurodegeneration on cognitive decline in clinically normal individuals. JAMA Neurol 2014;71:1379–1385.
2. Jack CR, Bennett DA, Blennow K, et al. A/T/N: an unbiased descriptive classification scheme for Alzheimer disease biomarkers. Neurology 2016;87:539–547.
3. Jones DT, Knopman DS, Gunter JL, et al. Cascading network failure across the Alzheimer's disease spectrum. Brain 2016;139:547–562.
4. Sheline YI, Raichle ME, Snyder AZ, et al. Amyloid plaques disrupt resting state default mode network connectivity in cognitively normal elderly. Biol Psychiatry 2010; 67:584–587.
5. Zhang HY, Wang SJ, Liu B, et al. Resting brain connectivity: changes during the progress of Alzheimer disease. Radiology 2010;256:598–606.
6. Damoiseaux JS, Prater KE, Miller BL, Greicius MD. Functional connectivity tracks clinical deterioration in Alzheimer's disease. Neurobiol Aging 2012;33:828.e819–828.e830.
7. Greicius MD, Srivastava G, Reiss AL, Menon V. Default-mode network activity distinguishes Alzheimer's disease from healthy aging: evidence from functional MRI. PNAS 2004;101:4637–4642.
8. Vlassenko AG, Vaishnavi SN, Couture L, et al. Spatial correlation between brain aerobic glycolysis and amyloid-β (Aβ) deposition. Proc Natl Acad Sci USA 2010;107: 17763–17767.
9. Elman JA, Madison CM, Baker SL, et al. Effects of beta-amyloid on resting state functional connectivity within and between networks reflect known patterns of regional vulnerability. Cereb Cortex 2016;26:695–707.
10. Villemagne VL, Burnham S, Bourgeat P, et al. Amyloid β deposition, neurodegeneration, and cognitive decline in sporadic Alzheimer's disease: a prospective cohort study. Lancet Neurol 2013;12:357–367.
11. Schultz AP, Chhatwal JP, Huijbers W, et al. Template based rotation: a method for functional connectivity analysis with a priori templates. Neuroimage 2014;102:620–636.
12. Buckner R, Roffman J, Smoller J. Brain Genomics Superstruct Project (GSP). Harv Dataverse 2014:10.
13. Holmes AJ, Hollinshead MO, O'Keefe TM, et al. Brain Genomics Superstruct Project initial data release with structural, functional, and behavioral measures. Sci Data 2015;2:150031.
14. Shaw EE, Schultz AP, Sperling RA, Hedden T. Functional connectivity in multiple cortical networks is associated with performance across cognitive domains in older adults. Brain Connect 2015;5:505–516.
15. Yeo T, Krienen FM, Sepulcre J, et al. The organization of the human cerebral cortex estimated by intrinsic functional connectivity. J Neurophysiol 2011;106:1125–1165.
16. Seeley WW, Menon V, Schatzberg AF, et al. Dissociable intrinsic connectivity networks for salience processing and executive control. J Neurosci 2007;27:2349–2356.
17. Andrews-Hanna JR, Reidler JS, Sepulcre J, Poulin R, Buckner RL. Functional-anatomic fractionation of the brain's default network. Neuron 2010;65:550–562.
18. Jones DT, Vemuri P, Murphy MC, et al. Non-stationarity in the "resting brain's" modular architecture. PLoS One 2012;7:e39731.
19. Buckner RL, Andrews-Hanna JR, Schacter DL. The brain's default network. Ann NY Acad Sci 2008;1124: 1–38.
20. Sperling RA, LaViolette PS, O'Keefe K, et al. Amyloid deposition is associated with impaired default network function in older persons without dementia. Neuron 2009;63:178–188.
21. Becker JA, Hedden T, Carmasin J, et al. Amyloid-β associated cortical thinning in clinically normal elderly. Ann Neurol 2011;69:1032–1042.
22. Price JC, Klunk WE, Lopresti BJ, et al. Kinetic modeling of amyloid binding in humans using PET imaging and Pittsburgh compound-B. J Cereb Blood Flow Metab 2005;25:1528–1547.
23. Mormino EC, Betensky RA, Hedden T, et al. Amyloid and APOE ε4 interact to influence short-term decline in preclinical Alzheimer disease. Neurology 2014;82: 1760–1767.
24. Donohue MC, Sperling RA, Salmon DP, et al. The preclinical Alzheimer cognitive composite: measuring amyloid-related decline. JAMA Neurol 2014;71:961–970.
25. Wechsler D, Stone CP. Wechsler Memory Scale-Revised. San Antonio, TX: Psychological Corporation; 1987.
26. Folstein MF, Folstein SE, McHugh PR. "Mini-mental state": a practical method for grading the cognitive state of patients for the clinician. J Psychiatr Res 1975;12: 189–198.
27. Wechsler D. WAIS-R Manual: Wechsler Adult Intelligence Scale-Revised. San Antonio, TX: Psychological Corporation; 1981.
28. Grober E, Lipton RB, Hall C, Crystal H. Memory impairment on free and cued selective reminding predicts dementia. Neurology 2000;54:827–832.
29. Mormino EC, Smiljic A, Hayenga AO, et al. Relationships between beta-amyloid and functional connectivity in different components of the default mode network in aging. Cereb Cortex 2011;1:2399–2407.
30. Myers N, Pasquini L, Göttler J, et al. Within-patient correspondence of amyloid-β and intrinsic network connectivity in Alzheimer's disease. Brain 2014;137: 2052–2064.
31. Hedden T, Van Dijk KRA, Becker JA, et al. Disruption of functional connectivity in clinically normal older adults harboring amyloid burden. J Neurosci 2009;29:12686–12694.

32. Buckner R, Sepulcre J, Talukdar T, et al. Cortical hubs revealed by intrinsic functional connectivity: mapping, assessment of stability, and relation to Alzheimer's disease. J Neurosci 2009;29:1860–1873.
33. Palop JJ, Mucke L. Amyloid-[beta]-induced neuronal dysfunction in Alzheimer's disease: from synapses toward neural networks. Nat Neurosci 2010;13:812–818.
34. Sperling RA, Aisen PS, Beckett LA, et al. Toward defining the preclinical stages of Alzheimer's disease: recommendations from the NIA-AA workgroups on diagnostic guidelines for Alzheimer's disease. Alzheimers Dement 2011;7:280–292.
35. Arenaza-Urquijo EM, Landeau B, La Joie R, et al. Relationships between years of education and gray matter volume, metabolism and functional connectivity in healthy elders. Neuroimage 2013;83:450–457.
36. Hedden T, Schultz AP, Rieckmann A, et al. Multiple brain markers are linked to age-related variation in cognition. Cereb Cortex 2016;26:1388–1400.
37. Stern Y. An approach to studying the neural correlates of reserve. Brain Imaging Behav 2017;11:410–416.
38. Drzezga A, Becker JA, Van Dijk KR, et al. Neuronal dysfunction and disconnection of cortical hubs in nondemented subjects with elevated amyloid burden. Brain 2011;134:1635–1646.
39. Ittner LM, Götz J. Amyloid-β and tau: a toxic pas de deux in Alzheimer's disease. Nat Rev Neurosci 2011;12:67–72.
40. Chatfield MD, Brayne CE, Matthews FE. A systematic literature review of attrition between waves in longitudinal studies in the elderly shows a consistent pattern of dropout between differing studies. J Clin Epidemiol 2005;58:13–19.

This Week's *Neurology*® Podcast

Intake of dairy foods and risk of Parkinson disease **(see p. 46)**

This podcast begins and closes with Dr. Robert Gross, Editor-in-Chief, briefly discussing highlighted articles from the July 4, 2017, issue of *Neurology*. In the first segment, Dr. Michelle Fullard talks with Dr. Katherine C. Hughes about her paper on intake of dairy foods and risk of Parkinson disease. In the second part of the podcast, Dr. Stacey Clardy focuses her interview with Dr. Dennis Bourdette on new immunotherapies in neurology.

Disclosures can be found at Neurology.org.

At Neurology.org, click on "RSS" in the Neurology Podcast box to listen to the most recent podcast and subscribe to the RSS feed.

CME Opportunity: Listen to this week's *Neurology* Podcast and earn 0.5 AMA PRA Category 1 CME Credits™ by answering the multiple-choice questions in the online Podcast quiz.

Succeed and Flourish in Your Practice with New Practice Leadership Program

Are you a US neurologist employed in a solo or small group practice? Develop and hone the kind of unique leadership skills needed to succeed and flourish in today's environment with the American Academy of Neurology's latest leadership program: Practice Leadership. We've designed a convenient program format specifically with your concerns about coverage and time away from practice in mind. Visit *AAN.com/view/PracticeLeadership* to learn more and apply by July 31, 2017.

Functional network integrity presages cognitive decline in preclinical Alzheimer disease

Rachel F. Buckley, Aaron P. Schultz, Trey Hedden, et al.

Neurology 2017;89;29-37 Published Online before print June 7, 2017
DOI 10.1212/WNL.0000000000004059